Modern Physics Letters B, Vol. 8, No. 24 (1994) 1461–1482

THE MECHANICAL ACTION OF LASER LIGHT ON RYDBERG ATOMS

G. ALBER, W. T. STRUNZ, AND O. ZOBAY
Fakultät für Physik, Universität Freiburg, D-79104 Freiburg i.Br., Germany

Received 12 July 1994

The momentum exchange between a standing wave laser field and an atomic center-of-mass is dominated by the internal dynamics of an atomic electron in the exciting laser field. Rydberg atoms are one of the simplest physical systems where the dependence of this radiative force on the electronic dynamics can be investigated in detail. The characteristics of the momentum transfer between an atomic center-of-mass and a standing wave laser field strongly depend on whether the "particle" or the "wave" aspect of the electronic dynamics prevail. In this review recent theoretical advances in the description of the mechanical action of laser light on Rydberg atoms are discussed. These advances have become possible by the application of semiclassical path integral techniques with respect to the electronic dynamics which clearly exhibit the "particle" and "wave" aspects of this momentum transfer.

1. Introduction

The pioneering experiments of Lebedev[1] and Nichols and Hull[2] have demonstrated clearly that light exerts pressure on material particles. The physical origin of this radiation-induced force is the exchange of energy and momentum between the electromagnetic field and matter. A well-known example is the scattering of electrons caused by a standing wave electromagnetic field which acts as a diffraction grating.[3] In this case the nonresonant nature of the interaction between electrons and the electromagnetic field implies that this effect is observable only at very high radiation power. In the optical frequency regime, however, the interaction between radiation and matter, i.e. atoms and molecules, is almost resonant. Thus, effects of the radiation-induced force are observable also in the case of low intensity radiation fields. This resonant character of the interaction in the optical frequency regime manifests itself, for example, in the large value of the scattering cross section of light by atoms or molecules which is of the order of an optical wavelength squared. Compared to this, the Thomson scattering cross section, which characterizes the (nonresonant) interaction between radiation and electrons, is of the order of the electron radius squared and is therefore vanishingly small. Early experiments measuring the influence of photon scattering on the atomic center-of-mass motion were performed by Frisch.[4] The development of coherent laser light sources has led to a rapid development in this field of research. Since then mechanical effects of

optical radiation on atoms have been studied systematically[5–7] and have been used, for example, for cooling atoms down to temperatures below 1 mK[8–10] or, in atom optical applications, for deflecting atomic beams in a controlled way.[11–18]

The mechanical action of laser light on atoms is characterized by the large difference in mass between a typical atomic nucleus and its electrons. This implies that to a good degree of approximation momentum can be transferred from a radiation field to the atomic center-of-mass only by excitation of the internal electronic degrees of freedom. The resulting correlation between the atomic center-of-mass motion and the dynamics of the electrons of the atom offers interesting perspectives for applications. On the one hand this correlation allows the atomic center-of-mass degrees of freedom to be manipulated in a controlled way and on the other hand it can be used to investigate the internal dynamics of atomic electrons via observation of the atomic center-of-mass motion. As far as laser-induced atomic excitation processes are concerned, up to now both experimental and theoretical work has concentrated mainly on cases in which only one or a few atomic energy eigenstates are excited near resonance. Under these circumstances a theoretical description of the mechanical action of laser light on atoms in terms of dressed states of the strongly coupled atom–field system and the corresponding effective potentials is convenient.[19,20]

The advent of short and powerful laser pulses within the last decade has stimulated numerous investigations on a different kind of atomic and molecular excitation processes, namely, processes in which a large number of atomic or molecular energy eigenstates are excited coherently.[21] Typically, nonstationary atomic or molecular quantum states are prepared which are well localized spatially in comparison with the extension of the relevant classically allowed region. Due to the large level density, in the case of Rydberg atoms, such coherent laser-induced excitation processes appear quite naturally, if Rydberg states are excited sufficiently close to a photoionization threshold from an initially prepared, energetically low lying bound state. In this case due to angular momentum selection rules the resulting electronic Rydberg wave packets are localized only with respect to the radial electronic coordinate. The angular coordinates of such an excited Rydberg electron are still delocalized. Two major mechanisms for preparing such a wave packet have been discussed so far:

(1) The energy eigenstates are excited coherently with the help of a short laser pulse whose (Fourier-limited) bandwidth exceeds the mean level spacing of the excited energy eigenstates.[22–24]
(2) In the case of a long laser pulse energy eigenstates are excited coherently by the mechanism of power broadening. This happens if the Rabi frequency, which characterizes the strength of the laser-induced transitions between the initial and final states, exceeds the mean level spacing of the excited states.[25] So far, in these investigations, effects on the atomic center-of-mass motion have been neglected.

In this review recent first theoretical investigations on the mechanical action of laser light on the center-of-mass motion of Rydberg atoms are discussed.[26–28] The motivation for considering Rydberg atoms in this context is threefold. First of all, Rydberg atoms are one of the simplest physical systems with a sufficiently high level density of the electronic degrees of freedom so that coherent laser-induced excitation processes occur naturally and are almost unavoidable in many practical situations. Secondly, Rydberg states exhibit many universal features so that the results obtained apply to a large class of systems including atoms and molecules. This is because effects originating from the positively charged ionic core which is formed by the nucleus and the residual electrons can be described by a few quantum defect parameters[29,30] only. Thirdly, due to the long lifetimes of Rydberg states, effects arising from the spontaneous emission of photons which destroy quantum coherence are negligible. This implies that the momentum exchange between an atom and a laser field is completely coherent.

This summary of recent theoretical work concentrates on the following main questions: How do the dynamics of an excited electronic Rydberg wave packet in the presence of a standing wave laser field influence the atomic center-of-mass motion? How can the mechanical action of laser light on atoms be described in this case theoretically in a convenient way? How is this theoretical description related to the traditional approach which is based on dressed states of the strongly coupled atom–field system and their corresponding effective potentials? In Sec. 2 the general theoretical framework is discussed. It is based on a *semiclassical path representation*[21,31] of relevant atomic transition probability amplitudes. Hence, in the spirit of a path integral approach, these amplitudes are represented as a sum of contributions associated with paths describing the classical motion of a bound excited Rydberg electron in the Coulomb potential of the positively charged ionic core. Within this general framework recent theoretical results[26,28] on the deflection of fast atoms by standing wave laser fields are discussed in more detail in Sec. 3.

2. Problem and Theoretical Framework

In this section a general theoretical framework for the description of the mechanical action of laser light on Rydberg atoms is developed. It is valid for arbitrary atomic center-of-mass velocities. In particular, it is shown that a semiclassical path integral approach in terms of probability amplitudes associated with the classical motion of a bound, laser-excited Rydberg electron on classical Kepler ellipses gives a practical theoretical description.[21,31] Furthermore, this approach gives direct physical insight into the elementary processes which lead to the transfer of momentum between a standing wave laser field and the atomic center-of-mass.

The mechanical action of laser light on atoms may be studied in atomic diffraction experiments of the type shown in Fig. 1. A beam of atoms with well-defined initial total momenta $\mathbf{P}_{\text{in}}$ crosses a standing wave laser beam which is described classically by the electric field strength $\mathbf{E}(\mathbf{x},t) = \epsilon\mathcal{E}(\mathbf{x})e^{-i\omega t} + \text{c.c.}$ (ϵ is the polari-

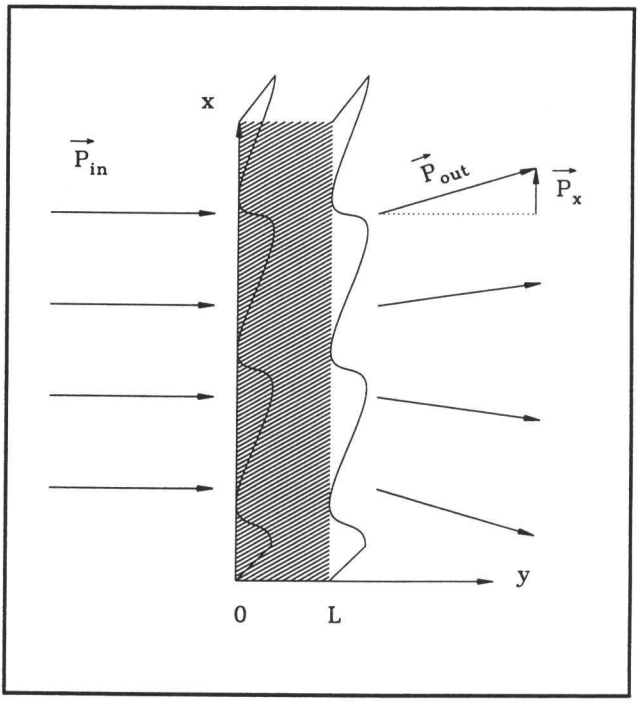

Fig. 1. Diffraction of an atomic beam by a standing wave laser field. The wavy lines indicate the standing wave laser field.

zation and ω is the frequency of the laser field). Initially all atoms of the beam are prepared in an energetically low lying bound electronic state. During the flight through the laser field an atom is excited to electronic Rydberg states close to the photoionization threshold. By this internal excitation process momentum is transferred from the laser field to the atomic center-of-mass and the atoms leave the interaction region in different directions $\mathbf{P}_{\text{out}}$.

Due to the large difference in mass between an atomic nucleus and its electrons, to a good degree of approximation, the direct influence of the laser field on the atomic center-of-mass motion can be neglected. Therefore, in the dipole approximation, the Hamiltonian, which describes the dynamics of an atom as it moves through the laser field, is given by

$$\hat{H} = \frac{\hat{\mathbf{P}}^2}{2M} + \hat{H}_A - \hat{\boldsymbol{\mu}} \cdot \mathbf{E}(\hat{\mathbf{x}}, t). \tag{1}$$

The atomic mass is denoted M, $\hat{\boldsymbol{\mu}}$ is the atomic dipole operator, and $\hat{\mathbf{P}}$ is the momentum operator associated with the atomic center-of-mass coordinate $\mathbf{x}$. The Hamiltonian $\hat{H}_{\text{A}}$ describes the internal dynamics of the atomic electrons in the Coulomb field of the atomic nucleus. In the following Hartree atomic units are used ("$e = \hbar = m_e = 1$").

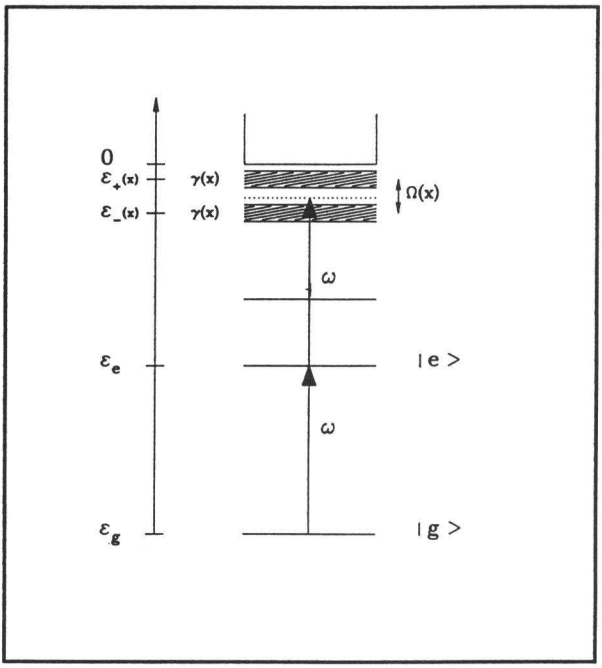

Fig. 2. Laser-induced electronic excitation process taking place during the flight of an atom through the standing wave laser field.

In view of the applications discussed in Sec. 3 let us consider the particular type of laser-excitation processes shown in Fig. 2 in more detail. Rydberg and continuum states close to a photoionization threshold are excited by the laser field $\mathbf{E}(\mathbf{x},t)$ from the energetically low lying bound state $|g\rangle$ or $|e\rangle$. These two bound states are assumed to be coupled almost resonantly by the laser field. Therefore, if the atoms are prepared in state $|g\rangle$ initially, the Rydberg states are excited by a two-photon process involving the intermediate resonant state $|e\rangle$. Alternatively, if the atoms are prepared in state $|e\rangle$, initially, and the laser-induced coupling to state $|g\rangle$ is negligible, this model describes the case of one-photon excitation of the Rydberg and continuum states. In the following effects of spontaneous emission of photons are neglected. This is valid as long as the interaction time between the atom and laser field is smaller than the lifetime of the bound state $|e\rangle$. Furthermore, we neglect ionization from the excited Rydberg states to continuum states well above threshold. For moderate laser intensities this is not a severe restriction (compare with condition (22)). In the optical frequency regime the small effects arising from Rydberg-continuum transitions may be taken into account by the inclusion of additional continuum channels which may be reached by radiative transitions.[25,32] Thus, the time evolution of the atomic state is approximately given by

$$\langle \mathbf{x}|\psi\rangle_t = a_g^{(t)}(\mathbf{x})|g\rangle + a_e^{(t)}(\mathbf{x})e^{-i\omega t}|e\rangle + \sum_n a_n^{(t)}(\mathbf{x})e^{-2i\omega t}|n\rangle. \tag{2}$$

Here, the sum over n indicates summation and integration over all bound Rydberg and continuum states close to threshold. The probability amplitudes $a_g^{(t)}(\mathbf{x})$,$a_e^{(t)}(\mathbf{x})$, and $a_n^{(t)}(\mathbf{x})$ of finding an atom at time t at position $\mathbf{x}$ in the state $|g\rangle$, $|e\rangle$, or $|n\rangle$ are determined by inserting Eq. (2) into the time-dependent Schrödinger equation with the Hamiltonian of Eq. (1). Assuming the laser field is turned on instantaneously at time $t = 0$ the resulting time-dependent Schrödinger equation can be solved with the help of the Laplace transform technique. Thus, for the Laplace-transformed amplitudes

$$a_j^{(z)}(\mathbf{x}) = \int_0^\infty dt e^{i(z+i0)t} a_j^{(t)}(\mathbf{x}), \tag{3}$$

the time-independent set of equations ($l = g, e$)

$$\sum_{j=g,e} \left[\left(z - \frac{\hat{\mathbf{P}}^2}{2M} \right) \delta_{l,j} - \mathcal{H}_{l,j} \right] a_j^{(z)}(\mathbf{x}) + \delta_{l,e} \sum_n \langle l|\boldsymbol{\mu} \cdot \boldsymbol{\epsilon}^* \mathcal{E}^*(\mathbf{x})|n\rangle a_n^{(z)}(\mathbf{x}) = i a_l^{(t=0)}(\mathbf{x}), \tag{4}$$

$$\left(z + 2\omega - \frac{\hat{\mathbf{P}}^2}{2M} - \epsilon_n \right) a_n^{(z)}(\mathbf{x}) + \langle n|\boldsymbol{\mu} \cdot \boldsymbol{\epsilon} \mathcal{E}(\mathbf{x})|e\rangle a_e^{(z)}(\mathbf{x}) = i a_n^{(t=0)}(\mathbf{x}) \tag{5}$$

is obtained in the rotating wave approximation. Here operators are indicated by a hat. The amplitudes $a_g^{(t=0)}(\mathbf{x})$, $a_e^{(t=0)}(\mathbf{x})$, and $a_n^{(t=0)}(\mathbf{x})$ represent the initial condition of an atom at time $t = 0$ when the laser field is turned on and the atom has not yet entered the interaction region. The Hamiltonian matrix

$$\mathcal{H}_{l,j} = \begin{pmatrix} \epsilon_g & , & -\langle g|\boldsymbol{\mu}\boldsymbol{\epsilon}^* \mathcal{E}^*(\mathbf{x})|e\rangle \\ -\langle e|\boldsymbol{\mu}\boldsymbol{\epsilon}\mathcal{E}(\mathbf{x})|g\rangle & , & \epsilon_e - \omega \end{pmatrix} \tag{6}$$

describes the dynamics of the bound states $|g$ and $|e\rangle$, which are coupled resonantly by the laser field.

If the Rydberg and continuum states close to the photoionization threshold are excited during the flight of an atom through the laser field, it is difficult to solve Eqs. (4) and (5) directly and to interpret the corresponding numerical solution in a simple, physically transparent way. In this case physical insight into the elementary processes which lead to momentum transfer from the laser field to the atoms is obtained by deriving semiclassical path representations for the state selective probability amplitudes $a_g^{(z)}(\mathbf{x})$ and $a_e^{(z)}(\mathbf{x})$. These amplitudes are expressed as a sum of probability amplitudes associated with possible classical paths of the excited Rydberg electron in the Coulomb field of the positively charged ionic core.[21,33] For this purpose Eq. (5) is inserted into Eq. (4). If the initial condition is such that $a_n^{(t=0)}(\mathbf{x}) = 0$, for example, we find

$$\sum_{j=g,e} \left\{ \left[\left(z - \frac{\hat{\mathbf{P}}^2}{2M} \right) \delta_{l,j} - \mathcal{H}_{l,j} - \hat{\Sigma}_{l,j}(\hat{\mathbf{x}}, z) \right] a_j^{(z)} \right\}(\mathbf{x}) = i a_l^{(t=0)}(\mathbf{x}). \tag{7}$$

The self-energy matrix of the bound states $|g\rangle$ and $|e\rangle$ is given by

$$\hat{\Sigma}_{l,j}(\hat{\mathbf{x}}, z) = \delta_{l,e}\delta_{j,e} \sum_n \langle n|\boldsymbol{\mu} \cdot \boldsymbol{\epsilon} \mathcal{E}(\hat{\mathbf{x}})|e\rangle^* \left(z + 2\omega - \frac{\hat{\mathbf{P}}^2}{2M} - \epsilon_n \right)^{-1} \langle n|\boldsymbol{\mu} \cdot \boldsymbol{\epsilon} \mathcal{E}(\hat{\mathbf{x}})|e\rangle. \tag{8}$$

In general, $\hat{\Sigma}(\hat{\mathbf{x}}, z)$ is a complicated nonlocal operator-valued function of $\hat{\mathbf{x}}$. With the help of quantum defect theory simple expressions may be derived in closed form which are the starting point for deriving a semiclassical path representation for the atomic amplitudes $a_g^{(z)}(\mathbf{x})$ and $a_e^{(z)}(\mathbf{x})$. Thus, as summarized in the Appendix, for an alkali atom with a (rigid) spherically symmetric core, for example, it is found that for $\mathrm{Im}\,(z) > 0$

$$a_l^{(z)}(\mathbf{x}) = i \sum_{j=g,e} ([\hat{U}_0(z) - i\Gamma \hat{U}_0(z)\mathcal{E}^*(\hat{\mathbf{x}})e^{2i\pi(\hat{\nu}+\alpha)} \times \sum_{N=1}^{\infty} (\hat{\tilde{\chi}}(\hat{\mathbf{x}}, z)e^{2i\pi\hat{\nu}})^{N-1}\mathcal{E}(\hat{\mathbf{x}})\hat{U}_0(z)]_{l,j} a_j^{(t=0)})(\mathbf{x}) \tag{9}$$

with

$$\hat{U}_0(z)_{l,j} = \left[z - \frac{\hat{\mathbf{P}}^2}{2M} - \mathcal{H} - \hat{\Sigma}^{(s)}(\hat{\mathbf{x}})\right]^{-1}_{l,j},$$

$$\hat{\Sigma}^{(s)}_{l,j}(\hat{\mathbf{x}}) = \delta_{l,e}\delta_{j,e}(\delta\omega - i\Gamma/2)|\mathcal{E}(\hat{\mathbf{x}})|^2,$$

$$\hat{\tilde{\chi}}(z)_{l,j} = \delta_{l,e}\delta_{j,e}\chi_c[1 - i\Gamma\mathcal{E}(\hat{\mathbf{x}})\hat{U}_0(z)_{e,e}\mathcal{E}^*(\hat{\mathbf{x}})],$$

and $\hat{\nu} = \int d^3P|\mathbf{P}\rangle\langle\mathbf{P}|[-2(z + 2\omega - \mathbf{P}^2/2M)]^{-1/2}$. The approximately energy-independent quantum defect of the Rydberg series is denoted by α and the scattering matrix element $\chi_c = e^{2i\pi\alpha}$ describes elastic scattering of the excited Rydberg electron off the spherically symmetric ionic core.

The physical significance of the terms on the right-hand side of Eq. (9) is straightforward[25,33]:

(1) The first term on the right-hand side of Eq. (9) is determined by the resolvent $\hat{U}_0(z)_{l,j}$. It describes the influence of the effective two-level system consisting of the resonantly coupled atomic states $|g\rangle$ and $|e\rangle$ on the atomic center-of-mass motion. The "smooth" part of the self-energy matrix $\hat{\Sigma}^{(s)}_{i,j}(\hat{\mathbf{x}})$ describes effects arising from the depletion of state $|e\rangle$ due to ionization. The quantities $\delta\omega|\mathcal{E}(\mathbf{x})|^2$ and $\gamma(x) = \Gamma|\mathcal{E}(\mathbf{x})|^2 = 2\pi|\langle\epsilon = 0|\boldsymbol{\mu}\cdot\boldsymbol{\epsilon}\mathcal{E}(x)|e\rangle|^2$ are, respectively, the quadratic Stark shift (due to virtual transitions between $|e\rangle$ and all other nonresonantly coupled atomic states) and the ionization rate from state $|e\rangle$ to the continuum states close to threshold (compare with the Appendix). Both quantities characterize the atom–laser interaction which is localized in a finite reaction zone extending typically only a few Bohr radii around the atomic nucleus.[32] As this reaction zone is small in comparison with the extension of highly excited Rydberg states these quantities are approximately independent of z[25,32] and the kinetic energy of the atomic center-of-mass $\mathbf{P}^2/2M$.

(2) The remaining terms on the right-hand side of Eq. (9) are probability amplitudes which are associated with repeated returns of an excited, bound Rydberg electron to the reaction zone. The Nth term describes the contribution of the

Nth return. The quantity $2\pi\langle\mathbf{P}|\hat{\nu}|\mathbf{P}\rangle$ is the classical action of a degenerate Kepler ellipse with zero angular momentum and energy $\epsilon = z + 2\omega - \mathbf{P}^2/2M$. With each return to the reaction zone an excited Rydberg electron is either de-excited to one of the bound states $|g\rangle$ or $|e\rangle$ by stimulated emission of a laser photon or it is scattered by the ionic core in the presence of the laser field. This latter laser-assisted electron–ion scattering process is described by the scattering operator $\hat{\tilde{\chi}}(z)$.[25]

Inverting the Laplace transform of Eq. (3) by

$$a_j^{(t)}(\mathbf{x}) = \frac{1}{2\pi}\int_{-\infty+i0}^{\infty+i0} dz e^{-izt} a_j^{(z)}(\mathbf{x}) \tag{10}$$

from Eq. (9) the semiclassical path representation of the time-dependent probability amplitudes $a_g^{(t)}(\mathbf{x})$, $a_e^{(t)}(\mathbf{x})$, and $a_n^{(t)}(\mathbf{x})$ is obtained. Although the semiclassical path representation allows one to split the state vector of the atom $\langle\mathbf{x}|\psi\rangle_t$ into contributions which originate from repeated returns of the excited Rydberg electron to the reaction zone, under general conditions, an explicit evaluation is still complicated. In the next section we study a special case of practical interest in which Eq. (9) can be simplified considerably and analytical expressions may be obtained for the state selective probability amplitudes $a_g^{(t)}(\mathbf{x})$ and $a_e^{(t)}(\mathbf{x})$.

3. Diffraction of Fast Atoms by a Standing Wave Laser Field

For the special case of fast atoms simple semiclassical path representations are available for state selective atomic transition probability amplitudes. They exhibit clearly the "particle" (wave packet) and "wave" (two-level) aspects of the momentum exchange between a standing wave laser field and the center-of-mass of an excited Rydberg atom. In particular, in resonant two-photon excitation processes "particle" and "wave" aspects of the electronic dynamics can influence the momentum exchange between a standing wave laser field and an atomic center-of-mass simultaneously.

If atoms which transverse a spatially modulated laser field at right angle as shown in Fig. 1 are fast enough, the eikonal approximation can be employed to describe the dynamics of the atomic center-of-mass motion.[19,20] In this approximation it is assumed that

(i)

$$\frac{P_{\text{in}}^2}{2M} \gg |\langle e|\boldsymbol{\mu}\cdot\boldsymbol{\epsilon}\mathcal{E}(\mathbf{x})|g\rangle|, |(\delta\omega - i\Gamma/2)|\mathcal{E}(\mathbf{x})|^2| \tag{11}$$

and

(ii)

$$\frac{P_x}{P_{\text{in}}} L \ll \lambda. \tag{12}$$

Conditions (11) and (12) imply that the operator of the kinetic energy $\hat{\mathbf{P}}^2/2M$ in Eq. (9) may be replaced by $\mathbf{P}_{\text{in}}^2/2M$. Furthermore, the Raman-Nath approximation[19,20] of Eq. (12) states that the total deflection of an atom during its way through the laser field is small in comparison with the wavelength of the laser field λ. Thus, to a good degree of approximation, the atomic center-of-mass moves with constant velocity on a straight line trajectory perpendicular to the momentum of the laser field.

In order to exhibit the basic physical aspects of the mechanical action of laser light on Rydberg atoms in more detail, in the following, an idealized, effectively two-dimensional scattering geometry is considered with the laser field approximated by

$$\mathcal{E}(\mathbf{x}) = \Theta(y)\Theta(L-y)\mathcal{E}(x). \tag{13}$$

Thus an atom experiences a constant electric field which is turned on and off instantaneously during its flight along the y direction and which depends on the position x along the standing wave where the atom crosses the laser field. The time of flight is given by $\tau = LM/P_{\text{in}}$.

3.1. *One-photon excitation of Rydberg states*

One-photon excitation of Rydberg states close to a photoionization threshold from an energetically low lying bound state can be described within the theoretical framework of Sec. 2 by considering the formal limit $\langle e|\boldsymbol{\mu}\cdot\boldsymbol{\epsilon}|g\rangle \to 0$ and assuming that initially the atom is prepared in state $|e\rangle$. As shown schematically in Fig. 2 the Rydberg and continuum states which are excited significantly by the laser field are located in the energy interval $(\epsilon_e+\omega-\Gamma|\mathcal{E}_0|^2, \epsilon_e+\omega+\Gamma|\mathcal{E}_0|^2)$ with $\mathcal{E}_0$ indicating the maximum value of the electric field strength of the standing wave $\mathcal{E}(x)$. Therefore, depending on the maximum intensity of the standing wave laser field, either one isolated or a large number of Rydberg states may be excited during the flight of an atom through the laser field.

3.1.1. *Excitation of an isolated Rydberg state*

If the laser intensity is sufficiently weak, only one isolated Rydberg state $|\bar{n}\rangle$ is excited almost resonantly by the laser field. This happens if the maximum field-induced excitation rate $\Gamma|\mathcal{E}_0|^2$, which characterizes the depletion of the initial state $|e\rangle$, is much smaller than the level spacing between adjacent Rydberg states, i.e.

$$\Gamma|\mathcal{E}_0|^2 \ll (\bar{n}-\alpha)^{-3}.$$

The quantum defect of the Rydberg states is denoted by α. Taking into account Eqs. (11) and (12) in this case the self-energy matrix of Eq. (8) may be approximated by

$$\hat{\Sigma}_{l,j}(\hat{\mathbf{x}},z) = \delta_{l,e}\delta_{j,e}\left(z+2\omega-\frac{\mathbf{P}_{\text{in}}^2}{2M}-\epsilon_{\bar{n}}\right)^{-1}|\langle\bar{n}|\boldsymbol{\mu}\cdot\boldsymbol{\epsilon}\mathcal{E}(\hat{\mathbf{x}})|e\rangle|^2. \tag{14}$$

Inserting Eq. (14) into Eq. (7) and inverting the Laplace transform the state selective transition amplitudes $a_e^{(\tau)}(x)$ and $a_{\bar{n}}^{(\tau)}(x)$ of finding an atom immediately after its flight through the laser field at position x in one of the internal states $|e\rangle$ or $|\bar{n}\rangle$ are evaluated easily. In the case of resonant excitation, i.e. $\epsilon_e + \omega = \epsilon_{\bar{n}}$, the well-known result[19,20]

$$e^{-i\omega\tau} a_e^{(\tau)}(x) = e^{-i(\epsilon_e + \mathbf{P}_{\rm in}^2/2M)\tau} \frac{1}{2} \left(e^{-i|\Omega(x)/2|\tau} + e^{i|\Omega(x)/2|\tau} \right) \tag{15}$$

is obtained with the time of flight τ and the Rabi frequency $\Omega(x) = 2\langle \bar{n}|\boldsymbol{\mu}\cdot\boldsymbol{\epsilon}\mathcal{E}(x)|e\rangle$. The two probability amplitudes on the right-hand side of Eq. (15) are associated with the two possible internal dressed states $|\pm\rangle$ of the strongly coupled two-level system $\{|e\rangle, |\bar{n}\rangle\}$. In the case of resonant excitation, as considered here, these dressed states are related to the "bare" atomic states $\{|e\rangle, |\bar{n}\rangle\}$ by

$$|\pm\rangle = \frac{1}{\sqrt{2}}(|e\rangle \pm |\bar{n}\rangle).$$

In the eikonal approximation (Eqs. (11) and (12)) the optical potentials

$$V_{\pm}^{\rm opt} = \pm\frac{1}{2}|\Omega(x)|,$$

which may be associated with these dressed states, lead to a spatial phase modulation of the state selective probability amplitude $a_e^{(\tau)}(x)$. The probability amplitude of observing a diffracted atom after its passage through the laser field with a momentum component P_x is obtained from Eq. (15) by Fourier transform, i.e.

$$a_e^{(\tau)}(P_x) = \frac{1}{\lambda}\int_0^{\lambda} dx e^{-ixP_x/\hbar} a_e^{(\tau)}(x). \tag{16}$$

Due to the periodicity of the standing wave laser field with wavelength λ only momentum components with $P_x = 2m\hbar k$ and $k = 2\pi/\lambda$ appear. Here, m denotes a positive or negative integer. Furthermore, the corresponding momentum distribution of the diffracted atoms is symmetric around $P_x = 0$. Thus, in the special case of a standing wave of the form $\mathcal{E}(x) = \mathcal{E}_0 \sin(kx)$, the well-known result[19,20]

$$a_e^{(\tau)}(P_x = 2m\hbar k) e^{-i\omega\tau} = J_{2m}(|\Omega_0|\tau/2) e^{-i(\epsilon_e + P_{\rm in}^2/2M)\tau} \tag{17}$$

is obtained with $\Omega_0 = 2\langle \bar{n}|\boldsymbol{\mu}\cdot\boldsymbol{\epsilon}\mathcal{E}_0|e\rangle$. Here, J_{2m} denotes the Bessel function of order $2m$. In Eq. (17) the appearance of even multiples of $\hbar k$ reflects the fact that for the observation of an atom in the initial state $|e\rangle$ an equal number of photon absorptions and stimulated emissions is required each of which transfers a momentum of magnitude $\pm\hbar k$ along the x-direction to the atomic center-of-mass. According to Eq. (17) the maximum momentum component which is transfered from the laser field to the atomic center-of-mass is approximately given by $P_x^{\rm max} = \pm\hbar k|\Omega_0|\tau/2$.

This traditional theoretical description of the mechanical action of laser light on atoms with the help of dressed states and their associated optical potentials[19,20] is convenient and physically appealing as long as only a few dressed internal atomic states are involved in the description of the laser excitation process. If a large number of Rydberg states are excited coherently during the flight of an atom through the laser field this approach becomes impractical. As discussed in the next section, in this case, a semiclassical path approach in terms of the classical paths of an excited Rydberg electron moving in the Coulomb field of the positively charged atomic core and their associated probability amplitudes is more convenient.

3.1.2. *Excitation of an electronic Rydberg wave packet*

A large number of Rydberg states are excited coherently during the flight of an atom through a laser field, if the maximum value of the field-induced excitation rate $\Gamma|\mathcal{E}_0|^2$ exeeds the level spacing between adjacent Rydberg states. This implies that a radial electronic Rydberg wave packet is excited. Such an electronic wave packet is a nonstationary quantum state of the excited Rydberg electron, which is well localized spatially in comparison with the large extension of highly excited Rydberg states. In the type of excitation process considered here this spatial localization takes place only with respect to the radial electronic coordinate. Due to angular momentum selection rules, which restrict the angular momentum of the excited Rydberg electron to low values, the angular coordinates of the laser-excited Rydberg electron are still delocalized.

The simplest case arises if the coherently excited Rydberg states are located energetically sufficiently well below the photoionization threshold and if the laser intensity is so small that a linear relation between the effective quantum number ν and the energy of the excited Rydberg electron may be assumed, i.e.

$$2\pi\hat{\nu} \approx 2\pi\bar{\nu} + T[z - \epsilon_e + \omega - P_{\text{in}}^2/(2M)]\,. \tag{18}$$

Here, $T = 2\pi\bar{\nu}^3$ with $\bar{\nu} = [-2(\epsilon_e + \omega)]^{-1/2}$ is the classical orbit time of a bound Coulomb orbit with energy $\epsilon_e + \omega < 0$ and zero angular momentum. This linearization is valid as long as effects of dispersion of the generated electronic Rydberg wave packet are negligible, i.e.

$$\left.\frac{d^2\nu}{dz^2}\right|_{\epsilon_e+\omega} (\Gamma|\mathcal{E}_0|^2)^2\tau \ll 1\,. \tag{19}$$

Furthermore, using the expansion

$$[\hat{\tilde{\chi}}(z)]_{l,j}^N = \delta_{l,e}\delta_{j,e}\chi_c^N \sum_{r=0}^{N} \binom{N}{r} [-i\Gamma\mathcal{E}(\hat{\mathbf{x}})\hat{U}_0(z)_{e,e}\mathcal{E}^*(\hat{\mathbf{x}})]^r\,,$$

we thus find from Eqs. (9) and (10) with the help of the residue theorem[27] the

semiclassical path representation

$$a_e^{(\tau)}(P_x)e^{-i\omega\tau} = e^{-i(\epsilon_e+\frac{P_{in}^2}{2M})\tau}\langle P_x|\Big[e^{-i(\delta\omega-i\Gamma/2)|\mathcal{E}(x)|^2\tau} + \sum_{N=1}^{\infty}\Theta(\tau-NT)e^{2i\pi(\bar{\nu}+\alpha)N}e^{-i(\delta\omega-i\Gamma/2)|\mathcal{E}(x)|^2(\tau-NT)} \times\sum_{r=0}^{N-1}\binom{N-1}{r}[e^{i\pi}\Gamma|\mathcal{E}(x)|^2(\tau-NT)]^{r+1}/(r+1)!\Big]|P_x=0\rangle\,. \quad (20)$$

Now the state selective probability amplitude $a_e^{(\tau)}(P_x)$ of finding an atom at time τ after the interaction with the laser field in the initial state $|e\rangle$ with momentum P_x along the direction of the standing wave is expressed as a sum of probability amplitudes associated with repeated collisions between an excited Rydberg electron and the atomic core in the presence of the laser field. These collisions take place during the flight of an atom through the laser field whenever the excited Rydberg electron approaches the atomic nucleus. They lead to a momentum transfer from the laser field to the atomic nucleus. The reaction zone around the atomic nucleus, within which these collisions take place, has a typical extension of a few Bohr radii. Therefore its diameter is small in comparison with the large extension of highly excited Rydberg states so that the atom–laser interaction may be viewed as spatially localized around the atomic nucleus.

The first term on the right-hand side of Eq. (20) describes the momentum transfer originating from the depletion of the initially prepared state $|e\rangle$. For interaction times $\tau < T$ it is the only contribution to $a_e^{(\tau)}(P_x)$. The special case of a standing wave laser field of the form $\mathcal{E}(x) = \mathcal{E}_0\sin(kx)$, for example, implies that in momentum space the matrix representation of the optical potential

$$V_{\text{opt}}(x) = (\delta\omega - i\Gamma/2)|\mathcal{E}(x)|^2$$

is proportional to the transfer matrix of an unbounded symmetrical random walk. Therefore this first term describes a random walk in momentum space with the complex-valued transition rate $(\Gamma/2 + i\delta\omega)|\mathcal{E}_0|^2/4$.[34]

The remaining terms on the right-hand side of Eq. (20) are associated with repeated returns of the excited Rydberg electron to the finite reaction zone around the atomic nucleus. According to Eq. (20) outside the reaction zone the excited Rydberg electron moves along one of the degenerate classical Kepler ellipses of zero angular momentum whose classical action is given by $S = 2\pi\bar{\nu}$. The additional phase contribution of magnitude $2\pi\alpha$ originates from elastic scattering of the excited Rydberg electron by the spherically symmetric ionic core.[29] The integer N counts the number of returns of the excited Rydberg electron to the reaction zone. The Heaviside function $\Theta(\tau - NT)$ ensures that the Nth term only contributes for interaction times $\tau > NT$. With each crossing of the reaction zone the laser-induced coupling between initial state $|e\rangle$ and excited states $|n\rangle$ is turned on and

off again. Thus, for a standing wave laser field of the form $\mathcal{E}(x) = \mathcal{E}_0 \sin(kx)$, two laser photons are exchanged during each of these laser-assisted electron–ion collisions by stimulated emission from the excited Rydberg states and subsequent photon absorption. Consequently the momentum of the center-of-mass of an excited atom is changed by an amount $\Delta P_x = 0$ or $\Delta P_x = \pm 2\hbar k$ along the x direction because these photons can have the same or opposite momenta of magnitude $\hbar k$. The (N, r)th term in Eq. (20) is the probability amplitude of the Nth return of the excited Rydberg electron to the reaction zone with a total number of r laser-assisted electron–ion scatterings during intermediate returns to the reaction zone. With each of these resonant scattering events the excited Rydberg electron experiences a time delay and a phase change of magnitude π. These effects are described by the factor

$$[e^{i\pi}\Gamma|\mathcal{E}(x)|^2(\tau - NT)]^r e^{-i(\delta\omega - i\Gamma/2)|\mathcal{E}(x)|^2(\tau - NT)} \tag{21}$$

in Eq. (20). The binomial coefficient $\binom{N-1}{r}$ is equal to the number of ways that r such scattering events can be selected from a total number of $(N-1)$ intermediate returns of an excited Rydberg electron to the reaction zone.

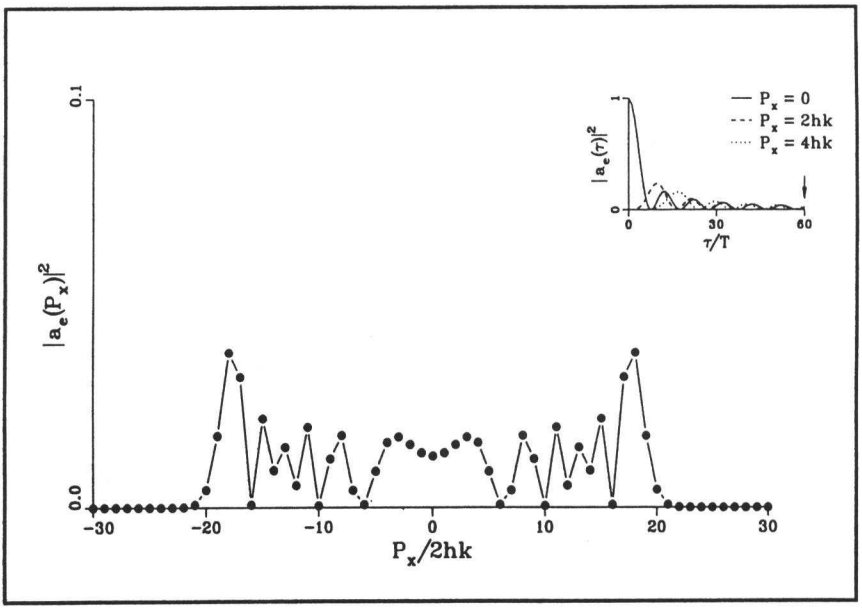

Fig. 3. Resonant one-photon excitation of an isolated Rydberg state: momentum distribution of $|a_e(\tau)|^2$ with $\Gamma|\mathcal{E}_0|^2 T = 0.1$, $\tau = 60T$. In the inset the time dependence of $|a_e(\tau)|^2$ is shown for $P_x = 0, 2\hbar k$, and $4\hbar k$.

Equation (20) gives a unified description of the momentum exchange between the atomic center-of-mass and the laser field. It is valid both in the two-level limit, if only one Rydberg state is excited significantly, i.e. $[\Gamma|\mathcal{E}_0|^2]^{-1} \gg T$, and in the opposite limit, if many Rydberg states are excited coherently, i.e. $[\Gamma|\mathcal{E}_0|^2]^{-1} \ll T$,

and an electronic wave packet is generated.[25,21] The two-level limit describes the "wave" aspect of the problem because in this case state selective probability amplitudes associated with almost all returns of an excited Rydberg electron to the reaction zone overlap in time and interfere. In Fig. 3 the probability of detecting an atom at time τ after the interaction with the laser field in its initially prepared state is shown as a function of momentum $P_x = 2m\hbar k$. In this case essentially only one Rydberg state is excited resonantly because $\Gamma|\mathcal{E}_0|^2T < 1$. Therefore Eq. (20) reduces to the well-known result of a resonantly excited two-level system as given in Eq. (17) with the Rabi frequency $\Omega_0 = \sqrt{\Gamma|\mathcal{E}_0|^2/T}$.[19] In the inset of Fig. 3 the time dependence of the initial state probability is shown for $P_x = 0, 2\hbar k$ and $4\hbar k$ as evaluated from Eq. (20). The corresponding results of the two-level limit of Eq. (17) are not shown as they are indistinguishable numerically. In particular, in this limit, $|a_e^{(\tau)}(P_x = 2m\hbar k)|^2$ changes slowly on the time scale T.

If an electronic Rydberg wave packet is generated, the "particle" aspect of the momentum transfer between atomic center-of-mass motion and laser field prevails because, at least for sufficiently small interaction times, probability amplitudes associated with repeated returns of the excited electron to the reaction zone are well separated in time. In Fig. 4 the initial atomic state $|e\rangle$ is depleted on a time scale

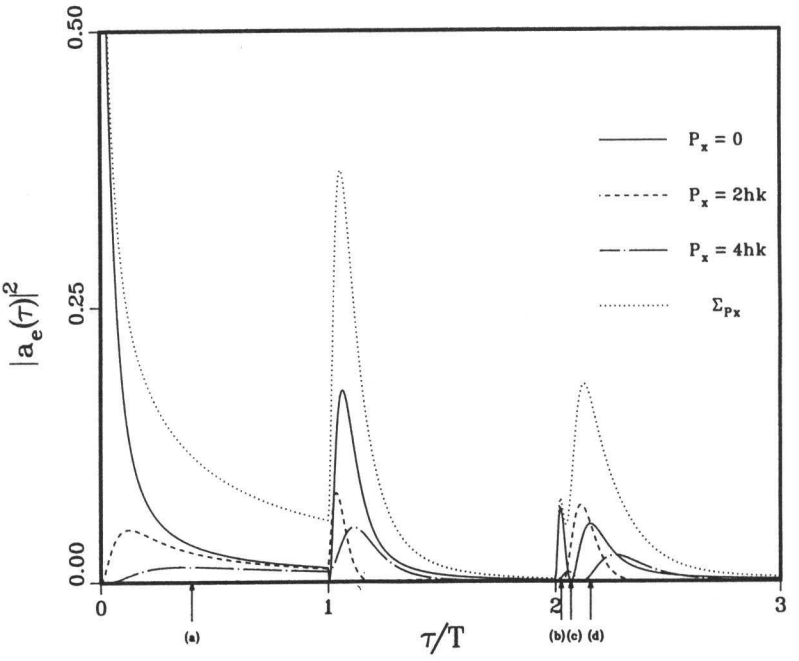

Fig. 4. Coherent one-photon excitation of Rydberg states: time dependence of $|a_e(\tau)|^2$ for $\Gamma|\mathcal{E}_0|^2T = 50$ and $P_x = 0$ (full curve), $2\hbar k$ (dashed curve), and $4\hbar k$ (dashed dotted curve). The dotted curve shows the total initial state probability (summed over all momentum components).

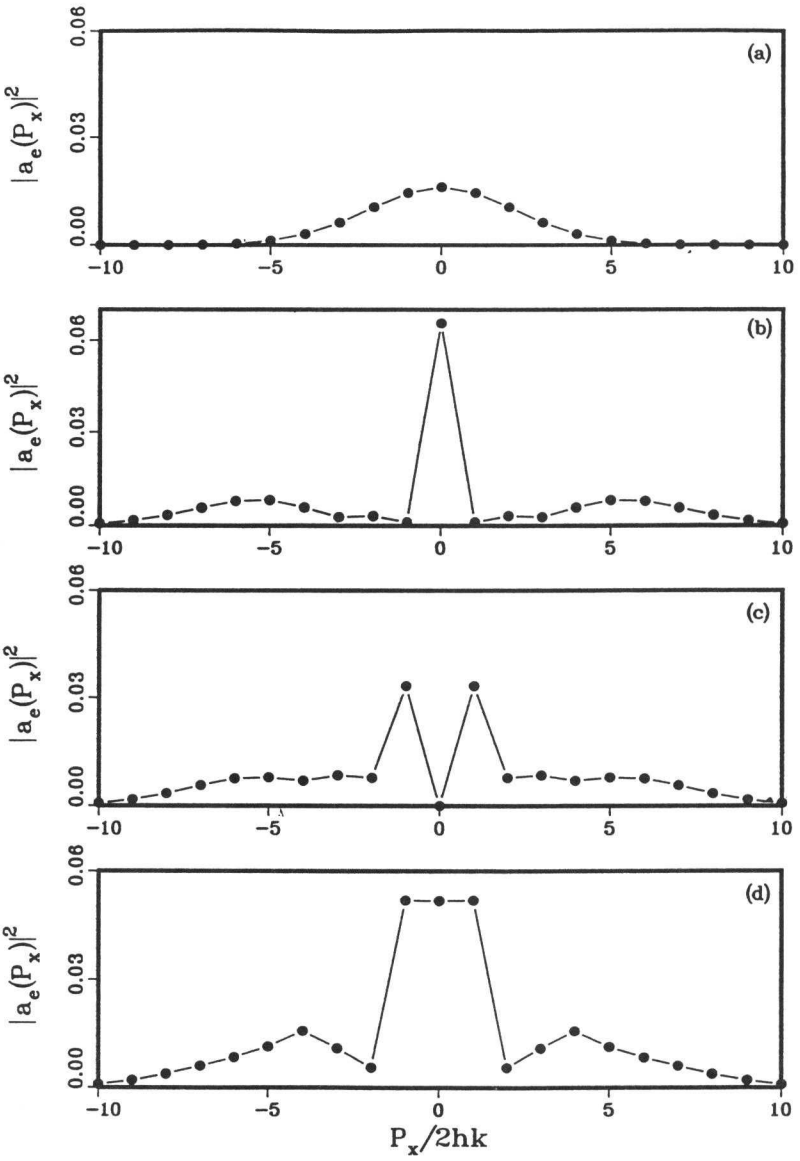

Fig. 5. Momentum distributions of $|a_e(\tau)|^2$ for the interaction times indicated by arrows in Fig. 4: (a) $\tau = 0.8 \times T$, (b) $\tau = 2.025 \times T$, (c) $\tau = 2.068 \times T$, (d) $\tau = 2.155 \times T$, and other parameters as in Fig. 4.

short in comparison with the mean classical orbit time of the excited Rydberg states, i.e. $[\Gamma|\mathcal{E}_0|^2]^{-1} < T$. Thus, a radial electronic Rydberg wave packet is generated by the laser-induced excitation process and the "particle" aspect of the momentum exchange between the center-of-mass motion of an excited atom and the laser field becomes apparent. This implies that a significant momentum transfer takes place

only at interaction times when the excited Rydberg electron is inside the reaction zone close to the atomic nucleus. The time evolution of the first few momentum amplitudes is shown in Fig. 4. In Figs. 5(a)–(d) momentum distributions for four different interaction times τ are shown, which are indicated by arrows in Fig. 4. These momentum distributions exhibit the diffusive character of the momentum transfer for $\tau < T$ (Fig. 5(a)) and the "particle" aspect of the momentum transfer for $\tau \approx 2T$ (Figs. 5(b)–(d)).

Finally we want to point out that in the model considered here ionization from the excited Rydberg states to the continuum states well above threshold has been neglected. This is valid as long as relevant interaction times τ are sufficiently small in the sense that[25,32]

$$\Gamma|\mathcal{E}_0|^2\tau/T \ll 1\,. \tag{22}$$

3.2. *Two-photon excitation of Rydberg states*

"Particle" (wave packet) and "wave" (two-level) aspects of the dynamics of an excited Rydberg electron can influence the momentum transfer between a standing wave laser field and the atomic center-of-mass motion simultaneously. This happens, for example, if Rydberg states close to a photoionization threshold are excited from an energetically low lying bound state via an intermediate resonant, bound state.[33] In this section basic physical aspects of the resulting mechanical action of laser light on the atomic center-of-mass motion are discussed within a simple model.

Let us consider again the idealized, effectively two-dimensional atomic beam deflection setup of Fig. 1. We assume that during the flight through the standing wave laser field an atom is excited from the initially prepared, energetically low lying bound state $|g\rangle$ to Rydberg states close to the photoionization threshold via an almost resonant, intermediate bound state $|e\rangle$ as shown in Fig. 2. The simultaneous presence of "particle" and "wave" aspects of the dynamics of an excited Rydberg electron is exhibited clearly, if the intermediate bound state $|e\rangle$ is excited resonantly, i.e. if $\epsilon_g + \omega = \epsilon_e$. Furthermore, let us assume that the Rabi frequency, which characterizes the laser-induced transition $|g\rangle \to |e\rangle$, is much larger than the excitation rate $\gamma(x) = \Gamma|\mathcal{E}(x)|^2$, which characterizes the depletion of the excited state $|e\rangle$. Under these conditions Rydberg states in energy intervals of width $\gamma(x)$ around the mean excited energies $\epsilon_\pm(x) = \bar{\epsilon} \pm |\Omega(x)|/2$ with $\bar{\epsilon} = \epsilon_g + 2\omega$ are excited significantly. These mean excited energies correspond to one-photon transitions from the dressed states $|\pm\rangle$ of the resonantly coupled bound states $|g\rangle$ and $|e\rangle$. In cases in which the excited Rydberg states are located sufficiently well below threshold so that effects of dispersion of a possibly excited electronic Rydberg wave packet are negligible (see Eqs. (18) and (19)), simple semiclassical path representations are obtained from Eqs. (9) and (10), namely,

$$a_g^{(\tau)}(x) = e^{-i(\epsilon_g + P_{\rm in}^2/2M)\tau} \frac{1}{2} \sum_{\pm} e^{\pm i|\Omega(x)|\tau/2} \Bigg[e^{-i[\delta\omega(x) - i\gamma(x)/2]\tau/2} + \sum_{N=1}^{\infty} \sum_{r=0}^{N-1} \binom{N-1}{r} \Theta[\tau - NT_{\pm}(x)] \times (\chi_c e^{2i\pi\bar{\nu}(x)_{\pm}})^N \frac{\{e^{i\pi}\gamma(x)[\tau - NT_{\pm}(x)]/2\}^{r+1}}{(r+1)!} \times e^{-i[\delta\omega(x) - i\gamma(x)/2][\tau - NT_{\pm}(x)]/2} \Bigg] \tag{23}$$

and a similar expression for $a_e^{(\tau)}(x)$. Here, the effective quantum numbers of the mean excited Rydberg states are denoted by $\bar{\nu}(x)_{\pm} = [-2\epsilon_{\pm}(x)]^{-1/2}$ and $T_{\pm}(x)$ are the classical orbit times of Kepler ellipses of zero angular momentum and energies $\epsilon_{\pm}(x)$. Due to the spatial variation of the laser field all these quantities depend on the position x at which an atom crosses the laser field. Equation (23) exhibits clearly the phase and amplitude modulations of the state selective transition amplitude $a_g^{(\tau)}(x)$ which are produced by repeated returns of an excited Rydberg valence electron to the reaction zone centered around the atomic nucleus.

The physical interpretation of the terms appearing in Eq. (23) is straightforward: Due to the ac Stark splitting between the resonantly coupled states $|g\rangle$ and $|e\rangle$, during the flight of an atom through the laser field, a Rydberg electron is excited either with mean energy $\epsilon_+(x)$ or $\epsilon_-(x)$. The probability amplitudes of these two pathways of excitation are denoted by the signs "$\pm$" in Eq. (23). The first term in square brackets on the right-hand side of Eq. (23) describes depletion of the initially prepared state $|g\rangle$ via these two pathways. The Nth term of the sum describes the contribution from the Nth return of an excited Rydberg electron to the reaction zone, which is localized spatially around the atomic nucleus. Inside this reaction zone the atom–laser interaction leads to the momentum transfer from the laser field to the atomic center-of-mass. With each return of the excited Rydberg electron to this reaction zone a stimulated transition to the strongly coupled bound states $|e\rangle$ and $|g\rangle$ may take place. This leads to an increase of the state selective probability amplitudes $a_g^{(\tau)}(x)$ and $a_e^{(\tau)}(x)$ at multiples of the mean classical orbit times $T_{\pm}(x)$ of the excited Rydberg states. As apparent from the Heaviside functions in Eq. (23) a contribution from the Nth return of an excited Rydberg electron with mean energy $\epsilon_{\pm}(x)$ can occur only if the time of flight of the atom through the laser field τ exceeds the N-fold of the corresponding mean classical orbit time. Furthermore, with each return to the reaction zone, a Rydberg electron may be scattered by the core in the presence of the laser field. The integer r enumerates these possible scattering events which may take place in the time interval τ between the initial excitation and final stimulated transition to one of the bound states $|e\rangle$ or $|g\rangle$. The binomial coefficient in Eq. (23) equals the number

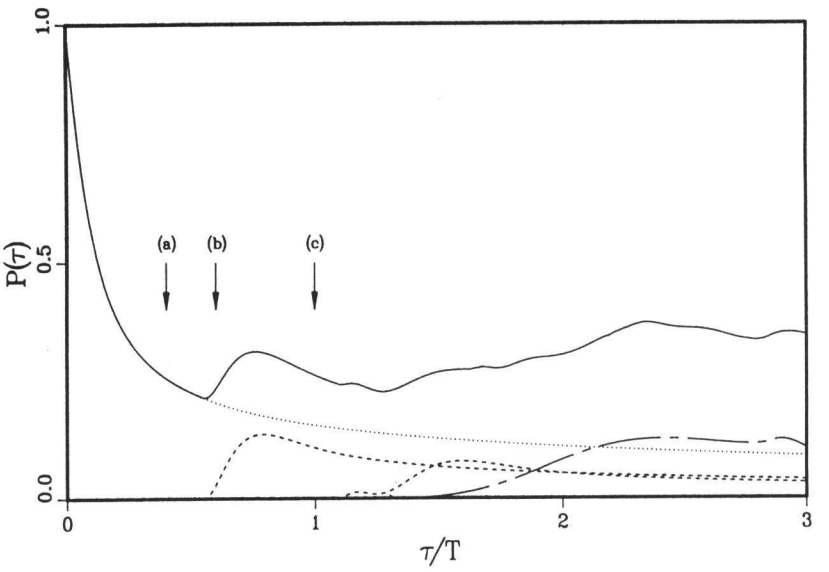

Fig. 6. Coherent one-photon resonant two-photon excitation of Rydberg states: time dependence of the total probability (summed over all momentum components) $|a_g(\tau)|^2 + |a_e(\tau)|^2$ for $\bar{\epsilon} = \epsilon_g + 2\omega = -10^{-5}$(a.u.), $T = 0.7 \times 10^8$(a.u.), $\Omega_0 = 10^{-5}$(a.u.), $\gamma_0 = 4 \times 10^{-7}$(a.u.), $\delta\omega(x) = 0$, and $\alpha = 0$.

of r-fold laser-assisted scattering events which are possible during N returns of the excited Rydberg electron to the reaction zone.

In Fig. 6 the time evolution of the probability of observing an atom after its flight through the laser field either in state $|g\rangle$ or $|e\rangle$ is shown (full curve). The laser field is assumed to be of the form $\mathcal{E}(x) = \mathcal{E}_0 \sin(kx)$ with Ω_0 and γ_0 indicating the maximum values of Rabi frequency and ionization rate, respectively. If an atom crosses the standing wave laser field at a position x at which the initial state $|g\rangle$ is depleted on a time scale small in comparison with the mean classical orbit times of the excited Rydberg states, i.e. $1/\gamma(x) \ll T_{\pm}(x)$, two radially localized electronic Rydberg wave packets with mean energies $\epsilon_{\pm}(x)$ are generated. The maxima appearing after the initial depletion of the bound states $|g\rangle$ and $|e\rangle$ in Fig. 6 are due to stimulated transitions of these electronic Rydberg wave packets to one of these bound states. These transitions take place during one of the subsequent returns of these wave packets to the reaction zone centered around the atomic nucleus. The remaining curves in Fig. 6 show the separate contributions of the initial depletion of states $|g\rangle$ and $|e\rangle$ (dotted curve), the first and second returns of the faster (dashed curves) and the first return of the slower (chain dashed curve) electronic Rydberg wave packet.

In Fig. 7 momentum distributions of atoms diffracted by the standing wave laser field are shown for three values of the time of flight τ which are indicated by arrows in Fig. 6. In Fig. 7(a) the interaction time τ between an atom and the laser field

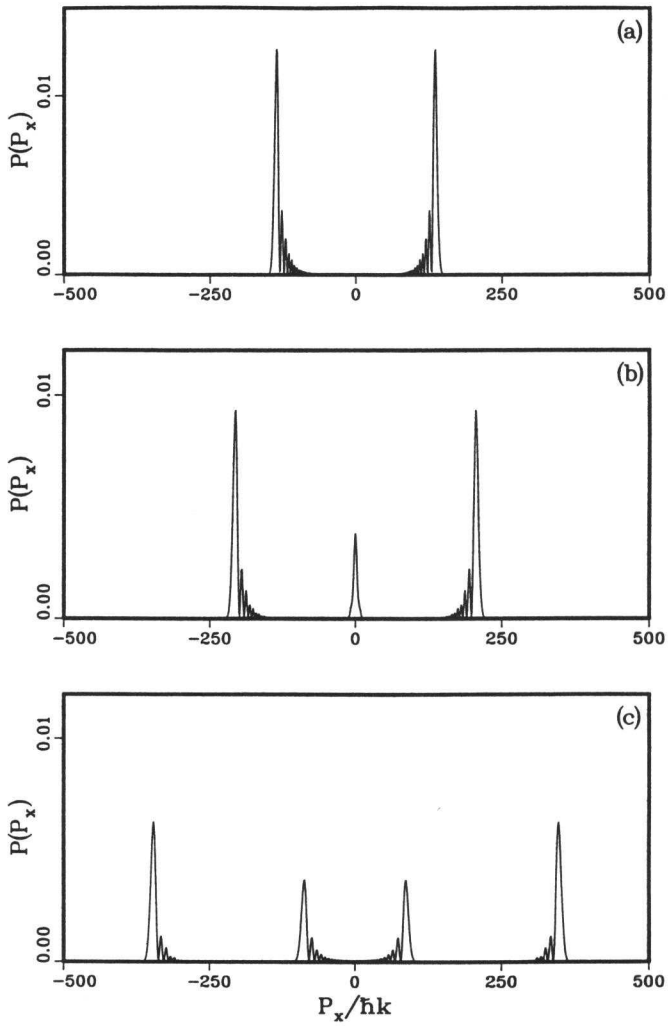

Fig. 7. Momentum distributions of $|a_g(\tau)|^2 + |a_e(\tau)|^2$ for the interaction times which are indicated in Fig. 5 by arrows. The other parameters are as in Fig. 6.

is so small that the electronic Rydberg wave packets have not yet returned to the atomic nucleus. Thus, the momentum distribution shows characteristic features of one-photon resonant two-photon ionization in a standing wave laser field. According to Eq. (23) the maxima of the momentum distribution appear approximately at the classical values $P_x = \pm(\hbar k)(|\Omega_0|\tau/2)$. It is the Rabi oscillations between the bound states $|g\rangle$ and $|e\rangle$ which lead to the large momentum transfer in this case. The widths of these maxima and the suppression of the oscillatory dependence on the transferred momentum, which is characteristic for two resonantly coupled states, originate from the depletion of the bound states $|g\rangle$ and $|e\rangle$.

In Fig. 7(b) the time of flight τ is sufficiently large so that the faster Rydberg wave packet with mean energy $\epsilon_-(x)$ and mean orbit time $T_-(x)$ has just returned to the atomic nucleus. Thus, the time $(\tau - T_-)$ available for stimulated transitions of this wave packet to one of the bound states $|g\rangle$ or $|e\rangle$ is not yet long enough to lead to a significant momentum transfer from the laser field to the atomic center-of-mass. Here, the quantity T_- is the smallest mean return time of all atoms which cross the laser field, i.e. $T_- = \min_x\{T_-(x)\}$. This implies that in the momentum distribution in addition to the maxima originating from the initial depletion process, a maximum centered around $P_x \approx 0$ also appears. A further increase of the time of flight leads to a splitting of this central maximum as shown in Fig. 7(c). Now four well-pronounced maxima appear in the momentum distribution of the diffracted atoms. The two outermost peaks are due to the initial depletion of the bound states. The central maxima now originate from the first return of the faster wave packet to the atomic nucleus. According to Eq. (23) these maxima appear at the classical values $P_x = \pm(\hbar k)[|\Omega_0|(\tau - T_-)/2]$, approximately.

The momentum distributions of Fig. 7 suggest the use of this excitation scheme, with the simultaneous presence of "particle" and "wave aspects" of the electronic dynamics, for a coherent atomic beam splitter which leads to a large momentum transfer.[28] According to Fig. 6 the efficiency of such a beam splitter is expected to be of the order of 30%. The practical feasibility of the model discussed here relies mainly on the validity of the Raman–Nath approximation (see Eq. (12)). However, in many practical cases, this condition is not a severe restriction and can be fulfilled by using sufficiently fast atoms and a sufficiently long wavelength of the standing wave laser field.[35–37]

4. Conclusion

The high level density of Rydberg states offers interesting perspectives for investigating effects of the electronic dynamics on the momentum transfer between standing wave laser fields and the atomic center-of-mass motion. Depending on whether contributions which correspond to repeated returns of an excited, bound Rydberg electron to the atomic nucleus (reaction zone) overlap in time or not, either the "wave" or the "particle" aspect of this momentum transfer prevails. Recently performed first theoretical studies, which have been reviewed here, show that semiclassical path representations are a convenient theoretical tool for describing the action of the resulting radiation-induced force on atoms. With the help of resonant multiphoton excitation of Rydberg states both the "wave" and "particle" aspects may determine the momentum transfer between a standing wave laser field and an atom simultaneously. This simultaneous presence of both complementary quantum aspects might have interesting applications, for example, for the realization of coherent atomic beam splitters.

Acknowledgements

This work was supported by the SFB 276 of the Deutsche Forschungsgemeinschaft.

Appendix

In this appendix the derivation of the general semiclassical path representation of Eq. (9) is outlined.

The main problem is the derivation of a semiclassical path representation for the self-energy matrix of Eq. (8). According to results of quantum defect theory,[29,30] close to threshold, the energy dependence of the dipole matrix elements in Eq. (8) is approximately given by

$$|\langle n|\boldsymbol{\mu}\cdot\boldsymbol{\epsilon}|e\rangle|^2 = |\langle \epsilon = 0|\boldsymbol{\mu}\cdot\boldsymbol{\epsilon}|e\rangle|^2 \left(\frac{d\epsilon_n}{dn}\right) \tag{A1}$$

with $\epsilon_n = -1/[2(n-\alpha)^2]$. Here, α denotes the quantum defect of the Rydberg series and $\langle \epsilon = 0|\boldsymbol{\mu}\cdot\boldsymbol{\epsilon}|e\rangle$ is an energy-normalized dipole matrix element to the continuum states close to threshold. To a good degree of approximation it is independent of energy. Using relation (A1) and the Poisson sum formula for performing the summation over all Rydberg and continuum states in Eq. (8), we obtain[25,27]

$$\hat{\Sigma}_{l,j}(\mathbf{x},z) = \delta_{l,e}\delta_{j,e}\int d^3P\mathcal{E}^*(\hat{\mathbf{x}})|\mathbf{P}\rangle\left(\delta\omega - i\Gamma/2 - i\Gamma\sum_{N=1}^{\infty} e^{2i\pi(\nu+\alpha)N}\right)\langle\mathbf{P}|\mathcal{E}(\hat{\mathbf{x}}) \tag{A2}$$

with $-1/(2\nu^2) = z + \omega - \mathbf{P}^2/2M$. This is the required semiclassical path representation for the self-energy matrix. The Nth term in the sum of Eq. (A2) may be interpreted as the contribution of the Nth return of a Rydberg electron of energy $\epsilon = -1/(2\nu^2)$ to the reaction zone centered around the atomic nucleus. The quadratic Stark shift $\delta\omega|\mathcal{E}(\hat{\mathbf{x}})|^2$, which is due to virtual transitions between state $|e\rangle$ and all other nonresonant atomic states, and the ionization rate $\Gamma|\mathcal{E}(\hat{\mathbf{x}})|^2$ are determined by the relation

$$\delta\omega - i\Gamma/2 = \int_{-\infty}^{\infty} d\epsilon|\langle\epsilon = 0|\boldsymbol{\mu}\cdot\boldsymbol{\epsilon}|e\rangle|^2\left(z + i0 + 2\omega - \frac{\hat{\mathbf{P}}^2}{2M} - \epsilon\right)^{-1}. \tag{A3}$$

Equation (9) is obtained upon substituting Eq. (A2) into Eq. (7).[25]

References

1. P. N. Lebedev, *Ann. Phys. (Leipzig)* **6**, 433 (1901); **32**, 411 (1910)
2. E. F. Nichols and G. F. Hull, *Phys. Rev.* **17**, 26, 91 (1903).
3. P. L. Kapitza and P. A. M. Dirac, *Proc. Cambridge Phil. Soc.* **29**, 297 (1933).
4. O. R. Frisch, *Z. Phys.* **86**, 42 (1933).
5. P. E. Moskowitz, P. L. Gould, S. R. Atlas, and D. E. Pritchard, *Phys. Rev. Lett.* **51**, 370 (1983).
6. P. L. Gould, G. A. Ruff, and D. E. Pritchard, *Phys. Rev. Lett.* **56**, 827 (1986).

7. P. J. Martin, B. G. Oldaker, A. H. Miklich, and D. E. Pritchard, *Phys. Rev. Lett.* **60**, 515 (1988).
8. S. Chu, L. Hollberg, J. E. Bjorkholm, A. Cable, and A. Ashkin, *Phys. Rev. Lett.* **55**, 48 (1985).
9. S. Chu, J. E. Bjorkholm, A. Ashkin, and A. Cable, *Phys. Rev. Lett.* **57**, 314 (1986).
10. C. Monroe, W. Swann, H. Robinson, and C. Wieman, *Phys. Rev. Lett.* **65**, 1571 (1990).
11. For a review of work on atom optics before 1992, see special issue of *Appl. Phys.* **B54**, 341ff (1992).
12. T. Pfau, Ch. Kurtsiefer, C. S. Adams, M. Sigel, and J. Mlynek, *Phys. Rev. Lett.* **71**, 3427 (1993).
13. S. N. Chormain, Ch. Miniatura, O. Gorceix, B. V. de Lesegno, J. Robert, S. Feron, V. Lorent, J. Reinhardt, J. Baudon, and K. Rubin, *Phys. Rev. Lett.* **72**, 1 (1994).
14. I. Sh. Averbukh, V. M. Akulin, and W. P. Schleich, *Phys. Rev. Lett.* **72**, 437 (1994).
15. J. Lawall and M. Prentiss, *Phys. Rev. Lett.* **72**, 993 (1994).
16. L. S. Goldner, C. Gerz, R. J. C. Spreeuw, S. L. Rolston, C. I. Westbrook, W. D. Phillips, P. Marte, and P. Zoller, *Phys. Rev. Lett.* **72**, 997 (1994).
17. M. Freyberger and A. M. Herkommer, *Phys. Rev. Lett.* **72**, 1952 (1994).
18. U. Janicke and M. Wilkens, *Phys. Rev. A*, in print.
19. A. P. Kazantsev, G. A. Ryabenko, and G. I. Surdutovich, *Phys. Rep.* **129**, 75 (1985).
20. A. P. Kazantsev, G. I. Surdutovich, and V. P. Yakovlev, *Mechanical Action of Light on Atoms* (World Scientific, Singapore, 1990).
21. G. Alber and P. Zoller, *Phys. Rep.* **199**, 231 (1991).
22. G. Alber, H. Ritsch, and P. Zoller, *Phys. Rev.* **A34**, 1058 (1986).
23. V. Engel, H. Metiu, R. Almeida, R. A. Marcus, and A. H. Zewail, *Chem. Phys. Lett.* **152**, 1 (1988).
24. Ch. Meier and V. Engel, in *Femtosecond Chemistry*, eds. J. Manz and L. Wöste (Verlag Chemie, Weinheim, 1994).
25. G. Alber and P. Zoller, *Phys. Rev.* **A37**, 377 (1988).
26. G. Alber, *Phys. Rev. Lett.* **69**, 3045 (1992); **70**, 2200 (1993).
27. G. Alber, *Laser Phys.* **3**, 682 (1993).
28. G. Alber and W. T. Strunz, *Phys. Rev. A*, in press.
29. M. J. Seaton, *Rep. Prog. Phys.* **46**, 167 (1983).
30. U. Fano and A. R. P. Rau, *Atomic Collisions and Spectra* (Academic, N.Y., 1986).
31. G. Alber, *Z. Phys.* **D14**, 307 (1989).
32. A. Giusti and P. Zoller, *Phys. Rev.* **A36**, 5178 (1987).
33. G. Alber, Th. Haslwanter, and P. Zoller, *J. Opt. Soc. Am.* **B5**, 2439 (1988).
34. N. G. van Kampen, *Stochastic Processes in Physics and Chemistry* (North-Holland, Amsterdam, 1981), p. 142ff.
35. T. Sleator, T. Pfau, V. Balykin, O. Carnal, and J. Mlynek, *Phys. Rev. Lett.* **68**, 1996 (1992).
36. R. G. De Voe, *Opt. Lett.* **16**, 1605 (1991).
37. D. M. Giltner, R. W. Mc Gowan, N. Melander, and S. A. Lee, *Opt. Commun.* **107**, 227 (1994).